Original Article

Reduction of Metal Artifacts Caused by Titanium Peduncular Screws in the Spine by Means of Monoenergetic Images and the Metal Artifact Reduction Software in Dual-Energy Computed Tomography

Luca Ceccarelli, Giulio Vara, Federico Ponti, Marco Miceli, Rita Golfieri[1], Giancarlo Facchini

Department of Diagnostic and Interventional Radiology, IRCCS Istituto Ortopedico Rizzoli, [1]Department of Radiology, IRCCS Azienda Ospedaliero-Universitaria Di Bologna, Via Albertoni, Bologna, Italy

Abstract

Objectives: To evaluate the reduction of metal artifacts in patients with titanium peduncular screws in the spine using (1) conventional images (CI), (2) virtual monoenergetic reconstructions (VMRs), and (3) VMR + Metal Artifact Reduction Software (VMR + MARS), with dual-energy computed tomography (DECT). **Materials and Methods:** Twenty-four patients with titanium peduncular screws in the spine were studied using a 64-channel DECT. During the postprocessing phase, the CI, the VMRs from 100 to 140 keV, and the VMR at 140 keV + MARS were synthesized. All the images were considered, and a quantitative evaluation was performed measuring the attenuation values (in terms of Hounsfield Units) with region of interest, in correspondence with the most hyperdense and hypodense artifacts. All the values were then compared. A qualitative evaluation, in terms of image quality and extent of artifacts, was also performed by two radiologists. **Results:** In quantitative terms, the 140 keV + MARS reconstruction was able to significantly reduce both bright and dark metal artifacts, compared to CI and to VMRs. The VMR was capable of significantly reducing both dark and bright artifacts, compared to CI. In qualitative terms, the VMR at 140 keV proved to be the best, compared to CI and VMR + MARS images. **Conclusions:** The VMR + MARS image reduces metal artifacts from titanium peduncular screws more than VMRs alone and CI. Furthermore, the VMR can decrease metal artifacts from a quantitative and a qualitative point of view. Combining information from VMRs and VMR + MARS images could be the best way to solve the issue of metal artifacts on computed tomography images.

Keywords: Artifacts, beam hardening, dual energy

Received on: 22-09-2021 **Review completed on:** 08-03-2022 **Accepted on:** 09-03-2022 **Published on:** 05-08-2022

Introduction

Peduncular screws are currently considered fundamental orthopedic devices for posterior instrumentation, permitting strong fixation and a high fusion rate,[1] and are used to correct many pathological conditions, such as traumatic or osteoporotic vertebral fractures, spinal stenosis, symptomatic spondylolisthesis, or spinal deformities.[2,3]

After spine surgery, 10%–40% of patients may develop the "Failed Back Surgery Syndrome": a clinical condition in which surgery has failed to solve the initial problem or a condition where symptoms persist, with no reference to the underlying cause.[2,4]

The syndrome could be caused by many conditions such as the mispositioning, displacement or breakage of screws, hematomas, infectious processes with possible abscesses, or a combination of them,[1,2] and imaging plays a key role in detecting these postoperative complications, allowing the correct diagnosis and therapy.[1]

Address for correspondence: Dr. Giulio Vara, Via Ernesto Masi 43, 40137, Bologna, Italy.
E-mail: giulio.vara@gmail.com

Access this article online

Quick Response Code:

Website: www.jmp.org.in

DOI: 10.4103/jmp.jmp_121_21

How to cite this article: Ceccarelli L, Vara G, Ponti F, Miceli M, Golfieri R, Facchini G. Reduction of metal artifacts caused by titanium peduncular screws in the spine by means of monoenergetic images and the metal artifact reduction software in dual-energy computed tomography. J Med Phys 2022;47:152-8.

In particular, the computed tomography (CT) detains a central role in evaluating the postoperative spine making the hardware, the cortical bone, the bone-hardware interface, and the eventual presence of hematomas or abscesses.[1,5]

However, the radiological evaluation of the postoperative column and the surrounding tissues is often made difficult by the presence of metal artifacts,[5] represented by marked hyperdense and hypodense bands or strikes on CT images, respectively, caused by two physical phenomena: (1) the beam-hardening[5-7] and (2) the photon starvation.[5,7,8]

The former is primarily represented by hyperdense streaks[5] and it is generated by the higher average energy transmitted, because of the increased absorption of lower energy photons compared to those with higher energy. The latter is shown as dark streaks, which are the consequence of a gap of information caused by photons unable to reach the detector through metals with high attenuation coefficients.[5,8]

The extent of artifacts is related to the composition of metal hardware, since they are smaller for less dense materials (titanium < stainless steel)[2,4,9] and to the thickness, size, orientation, and geometry of prosthesis.[10]

Some expedients are known to reduce metal artifacts, such as the higher tube voltage (kV) and tube current (mAs), the optimal reconstruction kernels, the narrow collimation, the increase of slice reconstruction thickness, and the use of multiplanar reconstructions, but some of these cannot always be used in clinical practice because of the increase in the radiant dose.[5,6]

In recent years, an effective method to reduce metal artifacts has been developed: the virtual monoenergetic reconstructions (VMRs) with the dual-energy CT (DECT).

The DECT, through the acquisition of images at two different energy levels according to different techniques (depending on the vendor),[11-13] is able to balance the two datasets, in the postprocessing phase. This allows to extrapolate a VMR, which represents the image as if it had been virtually acquired by a true monoenergetic X-ray beam of a certain value,[3,5,14] allowing to select the proper virtual voltage image to reduce the beam hardening phenomenon.[15,16]

Several metal artifact reduction (MAR) algorithms exist commercially.[15] During the postprocessing phase, it can correct the metal artifacts by segmentation and reconstruction based on a CT number threshold.[10] MARs may also replace the photon-starved regions with information derived from accurate projection measurements using material decomposition on the corrected projections and monoenergetic images.[16] The process usually takes less than a minute.

Because none of the above methods is known to completely eliminate the presence of metal artifacts on the CT image, the aim of our work was to investigate the reduction of metal artifacts, in patients with only titanium peduncular screws in the spine using (1) conventional images, (2) VMRs, and (3) VMR + MAR Software (VMR + MARS), with DECT, to identify the best acquisition settings to use when evaluating postoperative spine exams.

Materials and Methods

Patient selection

A total of 24 patients were included in our retrospective study, 15 of whom were women (62.5%) and 9 were men (37.5%); the average age was 37.1 years (ranging from 18 to 79 years). All patients had previously undergone spine surgery and all were carriers of titanium peduncular screws. The orthopedic hardware was located in the thoracic spine in five patients (20.8%) and in the lumbar spine in 19 patients (79.2%). No hardware was found at the cervical spine level.

All the procedures applied in this research were in accordance with the Helsinki Declaration as revised in 2013. The study was approved by the ethics board of our institute.

Image acquisition and reconstructions

All patients were investigated with a 64-channel DECT (Discovery 750 HD, GE Healthcare, Milwaukee, WI, USA) using the same standardized protocol with the following parameters: collimation of 40 mm; rotation time 0.5 s; fast kV-switching between 80 and 140 kVp; pitch 1.375:1; matrix 512 × 512; and tube current 640 mA.

For dose optimization, a dose modulation algorithm was applied in all patients.

The contrast medium had not been administered during the exams.

The CT data were transferred to a workstation (Advantage Workstation, version 4.7, GE Healthcare) for postprocessing. During the postprocessing phase, the VMRs from 100 to 140 keV (interval 10 keV) and the VMR at 140 keV + MARS (general electric (GE) proprietary MAR algorithm) reconstruction were synthesized by means of dedicated GSI software (AW VolumeShare 7, GE Healthcare).

Quantitative evaluation

The quantitative evaluation was performed by defining a region of interest (ROI) (always the same circlararea of 60 mm2) on the axial plane, corresponding to the sectional area of the metal bar. The attenuation values (in terms of Hounsfield Units [HU]) were obtained in correspondence with the most hyperdense and hypodense artifacts, considering (1) CI, (2) VMRs from 100 to 140 keV (10 keV interval), and (3) VMR at 140 keV + MARS (140 keV + MARS) reconstructions [Figure 1].

The ROI was then expanded subsequently expanded 2 times using the "Ring" tool to sample the neighboring tissues for mean HU values and to find the most hypo-hyperdense areas to sample the artifacts [Figure 2].

The points in which to place the ROIs were identified through the "Localize Max Value" function of LifeX[17] on the two outer rings for beam hardening artifacts; the same function

was used on the inverted CT series to locate the ideal point for photon starving.

The borders of the spinal canal were segmented by a single radiologist using LifeX on both the 140 KeV and the 140KeV images; areas, differences between shapes, and intersections between shapes were reported.

For a single case, a contrast map of the spinal canal was computed to explore the definition of the borders of the spinal canal.

All the attenuation values were calculated by one radiologist. Among the group of VMRs at different energy levels, the average attenuation values were compared and the VMR with the average attenuation value closer to zero (therefore with fewer artifacts) was selected, for both artifacts. Then, a comparison of the attenuation values between the selected VMR, the 140 keV + MARS image, and the CI was made, for both artifacts.

Qualitative evaluation

The qualitative evaluation was performed by other two radiologists, expert in musculoskeletal radiology, who blind examined (1) the CI, (2) the VMR at 140 keV, and (3) the 140 keV + MARS reconstruction, and assigned each of them a score of 1–4 according to a Likert scale (1 = severe artifacts with serious impediment to diagnostic evaluation, 2 = moderate artifacts with moderate impediment to diagnostic evaluation, 3 = mild artifacts with reduced diagnostic uncertainty, and 4 = no artifacts with fully diagnostic images) [Table 1], considering the peduncular screw, the spinal canal, and the paravertebral soft tissues as important diagnostic elements.

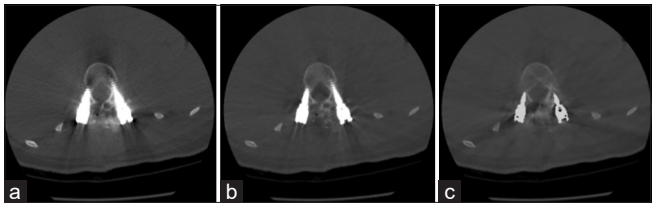

Figure 1: A 62-year-old male with titanium peduncular screws in the lumbar spine. The image shows the differences between the conventional image (a), the 140 keV virtual monoenergetic reconstruction (b), and the 140 keV + Metal Artifact Reduction Software reconstruction (c)

Statistical analysis

Values were expressed both as mean ± (standard deviation) and median (interquartile range,). Due to the sample size, the nonparametric Friedman test was used to compare the distribution of the attenuation values for the different images set. P <0.05 was considered statistically significant. For the qualitative evaluation, the interobserver agreement was calculated through a Fleiss weighted kappa test. A value of 0.20 was considered poor, 0.21–0.40 fair, 0.41–0.60 moderate, 0.61–0.80 good, and 0.81–1.00 excellent.

Results

Quantitative analysis

Neighboring tissues density

The average recorded HU value (+–DS) in the neighboring tissues to the metal bar was 93 (±124) HU in the inner ring, 61 (±94) HU in the middle ring, and 68(±101) HU in the outer ring.

Dark artifacts

By definition, the dark artifacts presented HU-negative values in CI. The quantitative analysis showed that in the group of VMRs, the one at 140 keV had the average attenuation value closest to zero (mean value: –85.6 ± 115.4 HU) [Table 2].

Bright artifacts

By definition, the bright artifacts presented HU-positive values in CI. For the bright artifact, the VMR at 140 keV showed the average attenuation value closest to zero (mean value: 134.4 ± 167.4 HU), compared to the other VMRs [Table 3].

Inferential analysis results and P values are reported in Table 4; the data are represented with a box plot [Figure 3].

Table 1: Likert scale for image quality evaluation

Likert scale	Description
1	Severe artifacts with serious impediment to diagnostic evaluation
2	Moderate artifacts with moderate impediment to diagnostic evaluation
3	Mild artifacts with reduced diagnostic uncertainty
4	No artifacts with fully diagnostic images

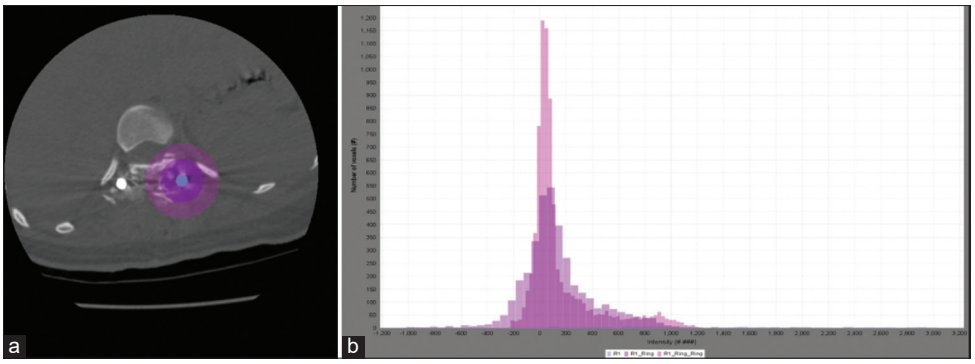

Figure 2: Sampling technique of the tissues surrounding the metal bar (a) and a histogram demonstrating their Hounsfield Units values (b)

Table 2: The mean value, the median value, the standard deviation and the 25-75 percentile f attenuation values (in terms of Hounsfield units) of dark artifacts, for each reconstruction

	Mean	Median	SD	25-75 *P*
100 keV VMR	−150.047	−122.005	121.0124	−189.850-−94.835
110 keV VMR	−125.932	−109.735	117.4494	−161.110-−63.730
120 keV VMR	−108.938	−101.045	115.9439	−145.890-−32.315
130 keV VMR	−95.896	−94.400	115.4155	−146.380-−8.520
140 keV VMR	−85.578	−89.155	115.3884	−142.195-5.955
140 keV + MARS	−11.058	−8.280	77.1867	−37.980-22.420
CI	−292.151	−262.135	157.1871	−371.335-−187.295

VMR: Virtual monoenergetic reconstruction, 140keV + MARS: Virtual monoenergetic reconstructions at 140 keV + Metal Artifact Reduction Software, SD: Standard deviation, CI: Conventional images

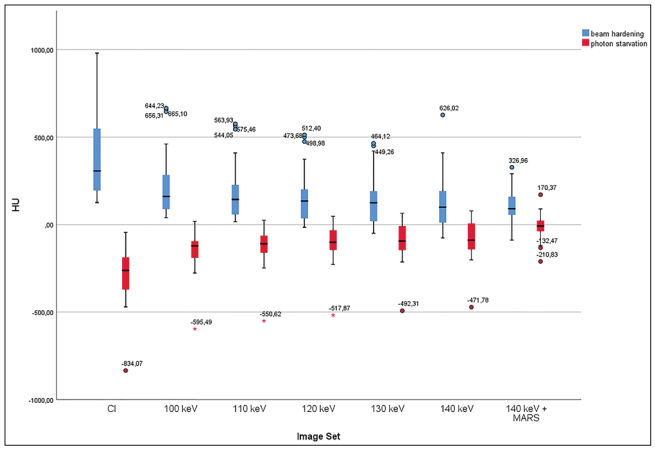

Figure 3: Attenuation values (in terms of Hounsfield Units) of hypodense artifacts in the 140 keV monoenergetic reconstructions (140 keV virtual monoenergetic reconstructions), in the 140 keV + Metal Artifact Reduction Software reconstructions and in conventional images conventional images. The Hounsfield Units -numbers of artifacts are significantly different among the different images

Spinal canal definition

The mean area on the spinal canal segmented on the 140 KeV images was 193 (±36) mm^2, while on 140 KeV was 206 (±51) mm^2 ($P = 0.1$). The mean difference between the areas was 43 (±22) mm^2, and the mean intersection was 173 (±34) mm^2.

Qualitative analysis

In all patients, the qualitative evaluation showed a better diagnostic quality of the VMR at 140 keV, compared to both CI and 140 keV + MARS reconstruction; this last one burdened by the presence of new artifacts introduced by the software. The interobserver agreement between the two radiologists was excellent (Kappa coefficient = 0.910) [Figures 4 and 5 and Table 5].

Discussion

In the postoperative spine evaluation of patients with metal peduncular screws, radiologists are often asked to verify the status or position of hardware or to investigate any presence of complications, such as hematomas or inflammation/infection with possible development of abscesses.[1]

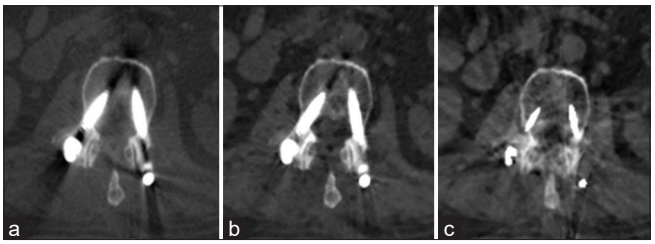

Figure 4: A 68-year-old male with titanium peduncular screws in the lumbar spine. The image shows the qualitative comparison between the conventional image (a), the virtual monoenergetic reconstruction at 140 keV (b), and the 140 keV + Metal Artifact Reduction Software reconstruction (c). The virtual monoenergetic reconstruction at 140 keV resulted to show fewer artifacts compared to the other two images. In this case, in the 140 keV + Metal Artifact Reduction Software reconstruction, the spinal canal was difficult to evaluate because of the marked presence of new artifacts introduced by the algorithm

The serious problem of metal artifacts that often overlap the bone, the spinal canal, and the paravertebral muscles, making visualization difficult and impaired, has been partially solved with some methods.

In recent years, DECT has established its role in reducing metal artifacts trough VMRs.[12,18] However, the optimal energy value for minimizing metal artifacts in each patient is variable and seems to depend on the system in use, the size, and composition of the orthopedic prosthesis.[12] A recent study has also shown that VMRs are more effective in reducing artifacts for small implants compared to bigger ones.[19] Zhou *et al*.[20] identified in the 130 keV the optimal photon energy setting with the lowest metal artifact for the total, internal, and external implanted metal orthopedic devices, in patients with fracture. In an *ex vivo* evaluation of posterior spinal fusion implants, Guggenberger *et al*.[21] demonstrated the effectiveness of VMRs in reducing artifacts and improving image quality, founding the range between 124 and 146 keV as the best energy interval to optimize the image quality with fewest artifacts. Studying 18 patients with scoliosis, similar results were founded by Wang *et al*.,[22] assessing that VMRs from DECT (GE Discovery CT 750 HD, GE Medical Systems) provided a superior image quality with reduced metal artifacts from titanium pedicle screws, compared to polychromatic images. Their optimal energy range was found to be between 110 and 140 keV.[22]

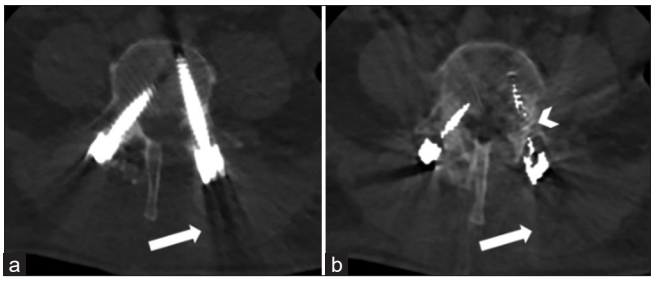

Figure 5: A 63-year-old male with titanium peduncular screws in the lumbar spine. The image shows the qualitative comparison between the 140 keV virtual monoenergetic reconstruction (a) and the 140 keV + Metal Artifact Reduction Software reconstruction (b). The dark artifacts at the level of paravertebral muscles (white arrow) were considered to be reduced in the 140 keV + Metal Artifact Reduction Software reconstruction compared to the 140 keV virtual monoenergetic image. However, in the 140 keV + Metal Artifact Reduction Software reconstruction the size of prosthesis was considered to be markedly underestimated (white arrowhead)

Another recent study[5] confirmed the efficiency of both high-keV VMRs and MAR algorithm (O-MAR, Philips Healthcare, Best, The Netherlands) in reducing metal artifacts caused by orthopedic hardware in the spine.

Following previous data in literature, we decided to analyze the VMRs at different energy levels in the range from 100 to 140 keV, with an interval of 10 keV. The average attenuation values closer to zero were found in the VMRs at 140 keV for both hyperdense and hypodense artifacts.

In accordance with previous results, in our study, we demonstrated that the highest monoenergetic reconstruction (at 140 keV) was able to reduce the artifacts (in terms of attenuation values in HU) from titanium peduncular screws more than CI for both dark artifacts and bright artifacts.

Moreover, with an excellent interobserver agreement between the two radiologists, the 140 keV-VMR was considered the best from a qualitative point of view, compared to both CI and 140 keV + MARS reconstruction. In fact, the VMR at 140 keV qualitatively presented reduced metal artifacts compared to CI, allowing an excellent visualization of the vertebral cortical bone, the screw bone interface, the spinal canal, and perivertebral soft tissues. Compared to the 140 kev + MARS reconstruction, the VMR at 140 keV was not affected by the presence of other new artifacts introduced by the algorithm, improving visualization.

The MARS is known to decrease the presence of metal artifacts, without an increase in the radiation dose, contrary to other methods.[10] Its potential in decreasing metal artifacts is due to the possibility to segment and reconstruct the image based on a CT threshold value during the postprocessing phase.[10] Even though the final reconstructed image still presents some artifacts, the image quality and the visualization of the periprosthesis region are considered generally improved.[10] Although this system can be used for different types of prostheses, it seems to be more effective for

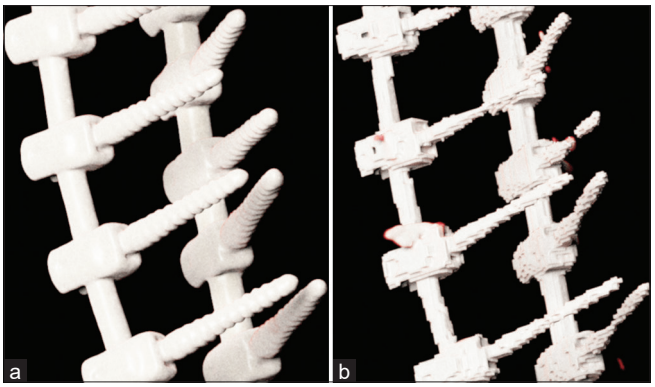

Figure 6: 3D rendering of a pedicle screw performed with 140 KeV images (a) and 140 KeV + Metal Artifact Reduction Software images (b)

Table 3: The mean value, the median value, the standard deviation and the 25-75 percentile of attenuation values (in terms of Hounsfield units) of bright artifacts, for each reconstruction

	Mean	Median	SD	25-75 *P*
100 keV VMR	224.287	160.945	196.2325	87.895-283.260
110 keV VMR	187.574	143.550	173.2779	57.340-226.715
120 keV VMR	161.552	134.670	159.6872	35.335-200.895
130 keV VMR	141.737	124.570	150.9871	18.845-190.570
140 keV VMR	134.418	99.625	167.4082	10.840-190.925
140 keV + MARS	108.317	90.010	90.0016	54.895-158.400
CI	401.236	306.105	258.6416	194.730-548.245

VMR: Virtual monoenergetic reconstruction, 140keV + MARS: Virtual monoenergetic reconstructions at 140 keV + Metal Artifact Reduction Software, CI: Conventional images, SD: Standard deviation

large prostheses (such as total knee arthroplasty or total hip arthroplasty) and for dense metal (cobalt-chrome or stainless steel instead of titanium).[10,16]

In 2018, while studying patients with spinal and hip prostheses, Park *et al*.[23] demonstrated that the combined use of VMRs and MAR-algorithm (O-MAR, Philips Medical System, The Netherlands) was able to reduce the image noise and to improve the image quality, compared to VMR and O-MAR applied alone. Despite the presence of new artifacts introduced by the algorithm in most cases (87%), the visualization of abdominal organs often resulted improved (85% of cases) with a subsequent reduction in false negatives and no significant impediment to the diagnostic value of the image.[23]

Our study proved that even in the case of titanium prostheses, the simultaneous use of 140 keV-VMR and MARS can reduce, albeit the result not being statistically significant, from a quantitative point of view, in terms of HU values, both bright and dark metal artifacts more than CI and high energy (140 keV)-VMR image.

Unlike the study conducted by Park *et al*.,[23] in our case, from a qualitative point of view in terms of diagnostic image quality and extent of artifacts, the 140 keV + MARS reconstruction did not result to be the best image. We justify this by the fact that MARS created the presence of new artifacts that had

Table 4: Results from the pairwise Friedman test comparing different images set for beam hardening and photon starvation artifacts

Pairwise Friedman test Beam hardening							
	100	110	120	130	140	140+ MARS	CI
100		1	0.018	<0.001	<0.001	0.008	1
110	1		1	0.044	<0.001	1	0.04
120	0,095	1		1		1	<0.001
130	<0.001	0.085	1		1	1	<0.001
140	<0.001	<0.001	0.062	1		0.192	<0.001
140+ MARS	<0.001	<0.001	0.005	0.529	1		<0.001
CI	0.683	0.008	<0.001	<0.001	<0.001	<0.001	

Photon starving. CI: Conventional images, MARS: Metal Artifact Reduction Software

Table 5: Results from the qualitative evaluation of the artifacts with the different imaging modalities, where 1 corresponds to hardly diagnostic presence of artifacts and 4 to good image quality

Inter-rater agreement			
	CI	140 KeV	140 KeV + MARS
Peduncular screw	3	4	1
Spinal canal	3	3	2
Paravertebral soft tissue	3	3	1

CI: Conventional images, 140keV + MARS: Virtual monoenergetic reconstructions at 140 keV + Metal Artifact Reduction Software

sometimes made it difficult to evaluate above all the spinal cord channel and the bone prosthesis interface [Figures 4 and 7].

In addition, the screw size was sometimes considered markedly underestimated and distorted by the two radiologist examiners [Figures 5 and 6].

In accordance with what previously recommended by other authors,[16] because of the presence of new artifacts introduced by MARS and the risk to underestimate the real size of prostheses, we suggest using MARS with caution and always comparing the reconstructed images with CI or VMRs, in order to avoid mistakes.

In the radiotherapy field, the extent of the effect of MAR algorithms is still being investigated: it has been demonstrated that the dependency of the efficacy of these algorithms in delineating tumoral contours are highly dependent on the geometry of the metal implants, whereas the dosimetric calculations do not statistically differ.[24,25] Considering this, MARs could be implemented in the suspect of the local recurrence of a spinal tumor.

Some limitations of our study should be mentioned. First of all, the retrospective nature of the study. In addition, the sample consisted of a relatively small number of patients, which could lead to a bias. However, since the data are statistically significant and encouraging, we believe that even with a larger sample, the same conclusions would be reached. Although the qualitative evaluation was blind conducted by the two radiologists, it was easy for them to identify where the MARS was applied, and this may have led to a bias. Since we did not investigate and evaluate the possible underlying pathological entities, but only the entity/extent of artifacts and the image quality, we believe that the study could be extended in the future considering and assessing the underlying pathologies in relation to the presence of metal artifacts.

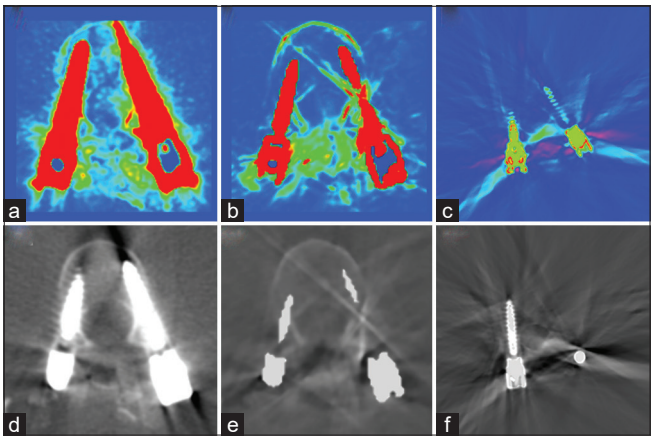

Figure 7: Contrast map of the 140 KeV and 140 KeV images (a and b) and the corresponding greyscale original (d and e), highlighting the different contours of the spinal canal. Subtraction images between the series showing the new artifact induced by the Metal Artifact Reduction and the faint contour of the spinal canal, present only in the 140 KeV images, displayed both in grayscale (f) and rainbow (c) for conspicuity of contrast

Furthermore, only the 140 keV VMR was postprocessed with the MARS, so the different effects of the algorithm were not explored on other VMRs; this decision was taken based on a preliminary analysis performed in the study design process and considering the existing literature, both showing that 140 keV is the best setting to reduce the artifacts.

Conclusions

In patients with titanium peduncular screws in the spine, the combined application of high energy VMR and MARS is able to reduce metal artifacts more than CI and high energy VMR alone, at least from a quantitative point of view. In addition, the high energy VMR (140 keV) significantly reduces metal artifacts compared to CI from a quantitative point of view. In

terms of image quality, the 140 keV-VMR could be considered better than both CI and 140 keV + MARS reconstruction, for the presence in the latter image of new artifacts introduced by the algorithm.

For the future, we recommend creating two datasets, with and without MARS, to have reference images to compare with. We believe that a comparative approach considering all the available images (VMRs and VMR + MARS reconstructions) could be the best method to reach the correct diagnosis. We think that by obtaining densitometric information from the VMR + MARS images and using the better diagnostic quality of the VMRs, radiologists could overcome the diagnostic challenge of metal artifacts.

Financial support and sponsorship

Nil.

Conflicts of interest

There are no conflicts of interest.

References

1. Hayashi D, Roemer FW, Mian A, Gharaibeh M, Müller B, Guermazi A. Imaging features of postoperative complications after spinal surgery and instrumentation. AJR Am J Roentgenol 2012;199:W123-9.
2. Douglas-Akinwande AC, Buckwalter KA, Rydberg J, Rankin JL, Choplin RH. Multichannel CT: Evaluating the spine in postoperative patients with orthopedic hardware. Radiographics 2006;26 Suppl 1:S97-110.
3. Srinivasan A, Hoeffner E, Ibrahim M, Shah GV, LaMarca F, Mukherji SK. Utility of dual-energy CT virtual keV monochromatic series for the assessment of spinal transpedicular hardware-bone interface. AJR Am J Roentgenol 2013;201:878-83.
4. Herrera Herrera I, Moreno de la Presa R, González Gutiérrez R, Bárcena Ruiz E, García Benassi JM. Evaluation of the postoperative lumbar spine. Radiologia 2013;55:12-23.
5. Große Hokamp N, Neuhaus V, Abdullayev N, Laukamp K, Lennartz S, Mpotsaris A, *et al*. Reduction of artifacts caused by orthopedic hardware in the spine in spectral detector CT examinations using virtual monoenergetic image reconstructions and metal-artifact-reduction algorithms. Skeletal Radiol 2018;47:195-201.
6. Lewis M, Reid K, Toms AP. Reducing the effects of metal artefact using high keV monoenergetic reconstruction of dual energy CT (DECT) in hip replacements. Skeletal Radiol 2013;42:275-82.
7. Barrett JF, Keat N. Artifacts in CT: Recognition and avoidance. Radiographics 2004;24:1679-91.
8. Shim E, Kang Y, Ahn JM, Lee E, Lee JW, Oh JH, *et al*. Metal artifact reduction for orthopedic implants (O-MAR): Usefulness in CT evaluation of reverse total shoulder arthroplasty. AJR Am J Roentgenol 2017;209:860-6.
9. Wellenberg RH, Donders JC, Kloen P, Beenen LF, Kleipool RP, Maas M, *et al*. Exploring metal artifact reduction using dual-energy CT with pre-metal and post-metal implant cadaver comparison: Are implant specific protocols needed? Skeletal Radiol 2018;47:839-45.
10. Lee YH, Park KK, Song HT, Kim S, Suh JS. Metal artefact reduction in gemstone spectral imaging dual-energy CT with and without metal artefact reduction software. Eur Radiol 2012;22:1331-40.
11. Agostini A, Borgheresi A, Mari A, Floridi C, Bruno F, Carotti M, *et al*. Dual-energy CT: Theoretical principles and clinical applications. Radiol Med 2019;124:1281-95.
12. Mallinson PI, Coupal TM, McLaughlin PD, Nicolaou S, Munk PL, Ouellette HA. Dual-energy CT for the musculoskeletal system. Radiology 2016;281:690-707.
13. Magarelli N, De Santis V, Marziali G, Menghi A, Burrofato A, Pedone L, *et al*. Application and advantages of monoenergetic reconstruction images for the reduction of metallic artifacts using dual-energy CT in knee and hip prostheses. Radiol Med 2018;123:593-600.
14. Murray N, Le M, Ebrahimzadeh O, Alharthy A, Mohammed MF, Ouellette HA, *et al*. Imaging the spine with dual-energy CT. Curr Radiol Rep 2017;5:44.
15. Huang JY, Kerns JR, Nute JL, Liu X, Balter PA, Stingo FC, *et al*. An evaluation of three commercially available metal artifact reduction methods for CT imaging. Phys Med Biol 2015;60:1047-67.
16. Pessis E, Sverzut JM, Campagna R, Guerini H, Feydy A, Drapé JL. Reduction of metal artifact with dual-energy CT: Virtual monospectral imaging with fast kilovoltage switching and metal artifact reduction software. Semin Musculoskelet Radiol 2015;19:446-55.
17. Nioche C, Orlhac F, Boughdad S, Reuzé S, Goya-Outi J, Robert C, *et al*. LIFEx: A freeware for radiomic feature calculation in multimodality imaging to accelerate advances in the characterization of tumor heterogeneity. Cancer Res 2018;78:4786-9.
18. Goo HW, Goo JM. Dual-energy CT: New horizon in medical imaging. Korean J Radiol 2017;18:555-69.
19. Kosmas C, Hojjati M, Young PC, Abedi A, Gholamrezanezhad A, Rajiah P. Dual-layer spectral computerized tomography for metal artifact reduction: Small versus large orthopedic devices. Skeletal Radiol 2019;48:1981-90.
20. Zhou C, Zhao YE, Luo S, Shi H, Li L, Zheng L, *et al*. Monoenergetic imaging of dual-energy CT reduces artifacts from implanted metal orthopedic devices in patients with factures. Acad Radiol 2011;18:1252-7.
21. Guggenberger R, Winklhofer S, Osterhoff G, Wanner GA, Fortunati M, Andreisek G, *et al*. Metallic artefact reduction with monoenergetic dual-energy CT: Systematic ex vivo evaluation of posterior spinal fusion implants from various vendors and different spine levels. Eur Radiol 2012;22:2357-64.
22. Wang Y, Qian B, Li B, Qin G, Zhou Z, Qiu Y, *et al*. Metal artifacts reduction using monochromatic images from spectral CT: Evaluation of pedicle screws in patients with scoliosis. Eur J Radiol 2013;82:e360-6.
23. Park J, Kim SH, Han JK. Combined application of virtual monoenergetic high keV images and the orthopedic metal artifact reduction algorithm (O-MAR): Effect on image quality. Abdom Radiol (NY) 2019;44:756-65.
24. Kwon H, Kim KS, Chun YM, Wu HG, Carlson JN, Park JM, *et al*. Evaluation of a commercial orthopaedic metal artefact reduction tool in radiation therapy of patients with head and neck cancer. Br J Radiol 2015;88:20140536.
25. Kovacs DG, Rechner LA, Appelt AL, Berthelsen AK, Costa JC, Friborg J, *et al*. Metal artefact reduction for accurate tumour delineation in radiotherapy. Radiother Oncol 2018;126:479-86.